Original Article

Fluoride Removal from Aqueous Solution Using Thermally Treated Dolomite Powder as Adsorbent in the Fixed Bed Column

Chinthayyanaidu Rudram[1,2], P. Dinesh Sankar Reddy[2,3]

[1]Department of Chemical Engineering, Rajiv Gandhi University of Knowledge Technologies, Nuzvid, Andhra Pradesh, India, [2]Department of Chemical Engineering, JNTUA College of Engineering, Ananthapuramu, Andhra Pradesh, India, [3]Department of Chemical Engineering, National Institute of Technology, Tadepalligudem, Andhra Pradesh, India

Abstract

Aim: The objective of this paper was to investigate the ability of thermally treated dolomite powder (TTDP) to remove fluoride ions from wastewater in a fixed bed column system, and to understand how different operating parameters such as bed height, initial fluoride concentration, and flow rate of influent affected the performance of the system. **Materials and Methods:** The researchers used several different models to analyze the data collected from the column experiments, and they also characterized the TDP adsorbent using field emission scanning electron microscopy and X-ray diffraction in order to understand its surface morphology. **Results:** Adsorption capacity increased with the initial fluoride concentration and decreased with bed height. Saturation concentration increases with an initial concentration of fluoride and decreases with bed height and flow rate of influent. Error analysis between experimental results and model results has been done using different predefined error functions. Regeneration of TDP adsorbent is done using a 1N NaOH solution. **Conclusions:** The breakthrough time increases with a low flow rate of 15 ml/min, low influent concentration of 5 ppm, and higher bed depth of 20 cm. The experimental data from the fixed bed column for fluoride removal are well fitted with all classic models, and the coefficient of regression is close to unity. Regeneration studies have shown that the adsorbent (TTDP) can undergo three cycles of regeneration.

Keywords: Adsorption process, dynamic model, error analysis, fluoride removal, regeneration, treated dolomite

Introduction

Fluorine is the 13th-most abundant element on the planet. Drinking water is the most common source of fluoride intake. It is a naturally occurring mineral that is typically found in both seawater and freshwater to some extent. It is primarily of geological origin and is found near the base of high mountains and in regions with volcanic eruptions and geothermal activities, such as natural hot springs. It can also be synthesized in laboratories and is often added to toothpaste, mouthwashes, and cosmetics. There are two well-known fluoride belts worldwide: one stretches from Turkey to Iraq, Afghanistan, Iran, Northern Thailand, India, and China, while the other runs from Syria to Jordan, Sudan, Algeria, Egypt, Libya, and Kenya.[1]

The presence of fluoride in the body can have either a positive or negative effect depending on its concentration and consumption. However, fluoride can interfere with the safety of drinking water supplies because it increases the risk of fluorosis with excessive intake. A significant amount of fluoride in water can protect teeth from decay, prevent cavities, and strengthen enamel. However, excessive fluoride intake can cause skeletal fluorosis or dental fluorosis, which damages the bones.[2]

According to the Indian Standard Drinking Water Specification of 1991 and the WHO 1984 guidelines, the fluoride content in drinking water should not exceed 1.5 ppm. Unfortunately, India is one of the 23 nations where health problems occur due to excess fluoride consumption. The states in India with high levels of fluoride are Andhra Pradesh, Punjab, Telangana, Tamil Nadu, Karnataka, Kerala, Delhi, Madhya Pradesh, and

Address for correspondence: Dr. Chinthayyanaidu Rudram, Rajiv Gandhi University of Knowledge Technologies, Nuzvid, Andhra Pradesh, India.
E-mail: chintu4407@gmail.com

Access this article online

Quick Response Code:

Website: www.ijehe.org

DOI: 10.4103/ijehe.ijehe_28_22

How to cite this article: Rudram C, Reddy PD. Fluoride removal from aqueous solution using thermally treated dolomite powder as adsorbent in the fixed bed column. Int J Env Health Eng 2024;13:13.

Received: 31-07-2022, **Revised:** 17-02-2023, **Accepted:** 17-04-2023, **Published:** 31-07-2024

Maharashtra. In around 20 states in India, it is estimated that more than 60 million people are drinking water that exceeds the permissible fluoride limit of 1.5 ppm. According to studies, the fluoride concentration in rural areas of India is 1.85 times higher than in urban areas. Using water with high levels of fluoride for irrigation can also lead to the accumulation of fluoride in food, posing a risk to adults and children in these areas. In addition to causing fluorosis, excess fluoride intake can also affect many processes in the body. As people age beyond 40 and pregnant women become more susceptible to calcium-related problems, the body's calcium requirements increase. The first step in addressing this problem is detection. Testing for fluoride content in water is a simple and affordable process. While detection does not prevent the problems caused by excess fluoride intake, it allows us to take action based on the concentration of fluoride present in a particular area and recognize its effects.[3]

To reduce health risks, it is recommended to use various techniques to remove fluoride from drinking water. For decades, defluoridation has been achieved through methods such as adsorption, ion exchange, reverse osmosis, nanofiltration, dialysis, and precipitation. Although there are many techniques available for removing fluoride, the choice of method depends on operating costs, requirements, and limitations. One of the popular methods is adsorption, as a wide range of adsorbents can be used depending on the specific needs. In precipitation and chemical additive methods, chemicals must be added to remove insoluble fluoride from the water, and these methods require further treatment to remove the additives. Reverse osmosis removes all minerals from the water, requiring remineralization to meet the minimum mineral requirements for drinking water. However, this method is not yet effectively developed for large-scale treatment purposes.[4]

From the survey of the literature, no data were available on the adsorptive removal of fluoride using dolomite ($CaMg[CO_3]2$) as an adsorbent. Dolomite has a double carbonate structure with an alternative arrangement of magnesium and calcium ions and is abundant in nature.[5] Most adsorption research is limited to batch trials, which do not provide appropriate scale-up data for large-scale treatment. The objective of this research was to investigate the effectiveness of a thermally treated dolomite powder (TTDP) column in removing fluoride ions from a fluoride-contaminated waste stream. The effects of bed depth, flow rate, and initial fluoride concentration on fluoride adsorption onto TDP were examined. To fit the experimental data, various models were employed, including the Bohart–Adam model, Thomas model, Clarke model, Wolbarska model, Yoon–Nelson model, and Yan model. Error analysis between experimental results and model results was performed using different predefined error functions. Batch regeneration studies of TDP were conducted using NaOH solution. The surface morphology of the adsorbents before and after treatments (BT and AT) with a fluoride aqueous solution was characterized using field emission scanning electron microscopy (FE-SEM) and X-ray diffraction (XRD).

Materials and Methods

Preparation of adsorbent

The waste of dolomite mines converted into powder was procured from the local market of Vijayawada. The powder was then sieved through sieve sizes of 41.5 µ. Then, the powder was thermally treated using a muffle furnace at 800°C for 2 h.

Preparation of stock solution

All the chemicals and reagents used in this investigation were of commercially available analytical grade (Fisher Scientific and Hanna Instruments). 2.21 g of sodium fluoride was added to 1 l deionized water to prepare a fluoride stock solution. This made 1000 ppm fluoride concentration in stock solution. This was diluted to concentrations of 2–20 ppm required for the experiments.[6]

Analysis and characterization

The concentrations of fluoride in synthetic solution were determined using fluoride high range, HI-98739 (Hanna Instruments). pH measurements were made with a digital pH Meter (ELICO - LI 617). XRD analysis and SEM characterization were made with the Ultra 55 model (Zesis made) and D8 Advance (Bruker made).[6]

Column studies

The experiments were carried out in a burette column with a 1 cm internal diameter and a 50 cm height. To maintain the desired flow rate, a peristaltic pump was used. To reduce adsorbent loss and provide mechanical support to the adsorbent bed, 1 cm thick wool was inserted on the bottom side. Experiments were conducted at a temperature of 35°C. Process factors such as flow rate (15, 18, and 20 ml/min), bed depth (5, 10, 15, and 20 cm), and concentration (5, 10, 15, and 20 ppm) were studied. Samples were taken every 2 min for the first 15 min, every 5 min for the next 45 min or 1 h, and then every 15 min or 30 min after 1 h from the top of the column and tested to determine the fluoride content. The schematic image of the continuous adsorption process and photographic image of the column are shown in Figures 1 and 2, respectively.[7]

Regeneration of adsorbent

Regeneration of adsorbent (saturated fluoride ions) was performed using different normality of NaOH (0.2N, 0.4N, 0.6N, 0.8N, 1N, and 1.2N). The fluoride-saturated adsorbent was suspended in 50 ml NaOH and shacked by a shaker at 200 RPM for 120 min. Again, the adsorbent was filtered out from the solution and dried for use in the adsorption process.[8]

Results

Column data analysis

The breakthrough behavior of the column adsorption process was investigated at different flow rates. The breakthrough curve was obtained with a constant influent concentration of 15 ppm and a bed height of 20 cm at flow rates of 15, 18, and 20 ml/min. The breakthrough time and exhaustion time for fluoride adsorption onto dolomite adsorbent decreased as the flow rate increased from 15 to 20 ml/min, as shown in Figure 3.

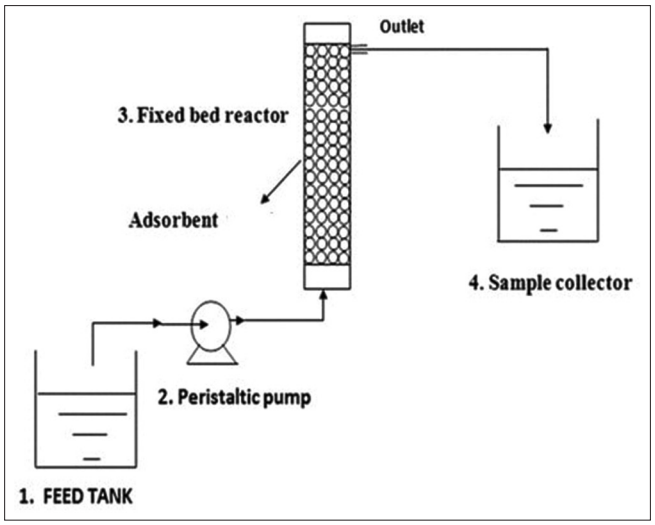

Figure 1: Schematic diagram of continuous column for adsorption of fluoride in aqueous solution

Figure 2: Photographic image of continuous column for adsorption of fluoride in aqueous solution in our laboratory

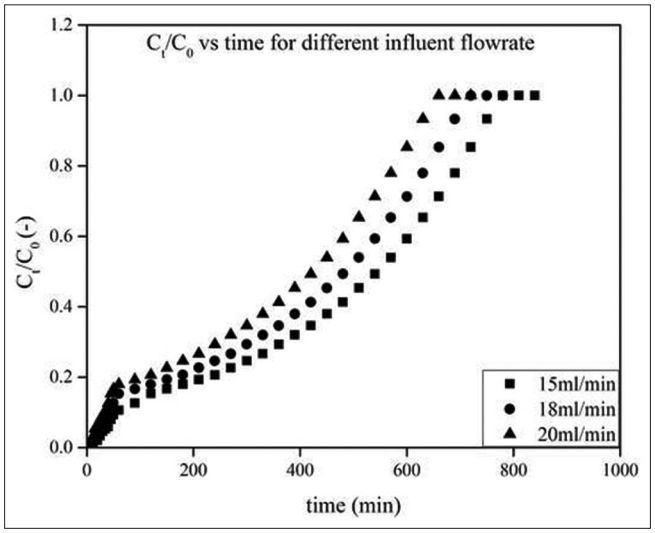

Figure 3: Effect of influent flow rate of fluoride solution on breakthrough curve

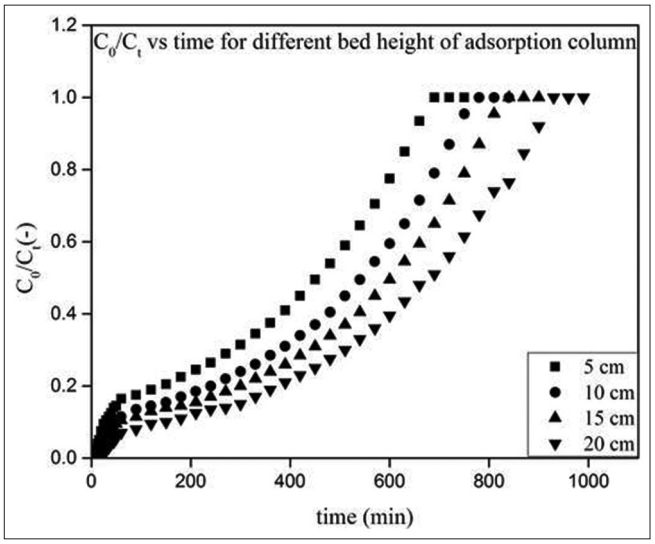

Figure 4: Effect of bed height of adsorption column on breakthrough curve

Figure 4 displays breakthrough curves obtained at different bed depths (5 cm, 10 cm, 15 cm, and 20 cm) with a constant influent concentration of 20 ppm and flow rate of 15 ml/min. As the bed depth increased, the breakthrough and exhaustion times also increased, as shown in the diagram.

Figure 5 illustrates the significant impact of the initial fluoride ion concentration on breakthrough. The breakthrough time was found to decrease as the influent fluoride concentration increased. At lower influent fluoride concentrations, breakthrough occurred more slowly, leading to more gradual breakthrough curves.

To design a successful column adsorption process, it is crucial to predict the concentration-time profile, or breakthrough curve, of the effluent. Various models, including the Bohart–Adam model, Thomas model, Clark model, Wolbarska model, Yoon–Nelson model, and Yan model, have been utilized to develop kinetic models for the column and estimate breakthrough curves. These models are useful in describing the behavior of fixed bed columns and can be scaled up for industrial applications.[8]

Thomas model

The Thomas model is the most widely used model for plotting breakthrough curves in fixed-bed adsorption at varying flow rates, bed depths, and influent concentrations. Thomas's model is accurate and gives best-fit results in conditions where internal and external resistances are extremely small. This model makes some assumptions to predict the breakthrough curves.[9] They are,

i. Plug flow is observed during the adsorption process
ii. With no axial dispersion at the solid/solution interface, mass transfer limits adsorption
iii. Experimental data follow the Langmuir isotherm
iv. This model follows second-order reversible kinetics.

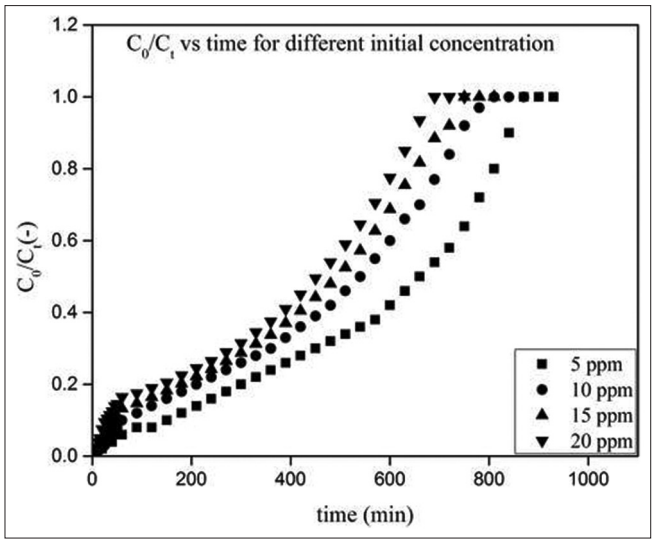

Figure 5: Effect of influent concentration of fluoride on fluoride removal breakthrough curve

It is shown in Equation 1.[10]

$$\frac{C_t}{C_0} = \frac{1}{1+\exp(\frac{K_{Th}q_0 m}{Q} - K_{Th}C_0 t)} \quad (1)$$

where K_{Th} is the second-order rate constant also called as Thomas constant (l/min. mg), q_0 is adsorption capacity (mg/g), m is the adsorbent mass (g), and C_0 is the initial influent concentration (ppm) and Q is the volumetric flow rate of influent.

Bohart–Adams model

Bohart–Adams devised a formula for calculating the size of a carbon adsorption column. The adsorption rate is assumed to be proportional to the residual adsorption capacity of the adsorbent and the concentration of adsorbate in this model. This model produces accurate findings in the early stages of the breakthrough curve. The Bohart–Adams model looks like Equation 2.[9]

$$\frac{C_o}{C_t} = \exp\left(K_{BA}C_o t - \frac{K_{BA}N_o z}{u_o}\right) \quad (2)$$

where K_{BA} - Bohart–Adams kinetic constant (L/min/mg), N_0 - the saturation concentration of adsorbate bed (ppm), C_0 is the initial concentration of influent (ppm), and z is bed height (m).

Yoon–Nelson model

Yoon–Nelson devised a basic and straightforward model for a single-component system. It does not necessitate specific information about the adsorbates, the type of adsorbent, or the physical parameters of the adsorption bed. The rate of decrease in adsorption for each adsorbate is assumed to be proportional to the adsorption and probability of breakthrough in this model.[9] The Yoon–Nelson model is written as Equation 3:[3]

$$\frac{C_t}{C_0} = \frac{1}{1+\exp(K_{yn}(\tau - t))} \quad (3)$$

where K_{yn} is the rate constant (time^{-1}) also called as Yoon–Nelson constant, τ is the time required for a 50% breakthrough, and C_0 is the concentration in the influent.

Clarke model

Clarke made some assumptions to develop the equation. They are,

i. Adsorption process here follows Freundlich isotherm
ii. Mass balance has been done over the whole column including all the exit solute streams over the column
iii. Mass balance equation for the liquid phase has developed by involving mass transfer concepts.

The Clarke model is revealed in Equation 4.

$$\frac{C_t}{C_0} = \frac{1}{1+A\exp(-rt)^{\frac{1}{n-1}}} \quad (4)$$

where A and r (time^{-1}) are the Clarke constants and n is the constant evaluated using the Freundlich isotherm.

Wolborska model

By the application of general mass transfer equations, a simplified model is proposed by Wolborska. It is mainly based on the diffusion mechanism within the range of lower concentrations of breakthrough curves. Adsorption of P-nitrophenol on activated charcoal has been conducted by Wolborska in a fixed bed column to validate his model. Empirical relation is given as Equation 5.[9]

$$\frac{C_t}{C_0} = \exp\left(\frac{\beta_a C_o t}{N_0} - \frac{\beta_a Z}{u_0}\right) \quad (5)$$

where, $ß_a$ is external mass transfer kinetic coefficient (h $-$ ^{1}), N_0 is Exchange capacity at saturation condition (mg/L), u_0 is Fluid superficial velocity in column (mm/h), Z is Height of the fixed adsorption bed (mm).

The Yan model

This model is proposed based on the statistical analysis of results obtained from the experiments conducted. Some modifications and simplifications were made during the validation with the obtained data. In comparison with all other models, the YAN model is more reliable as it gives a detailed explanation of the breakthrough curve precisely. The empirical relation is given in Equation 6,

$$\frac{C_t}{C_0} = 1 - \frac{1}{1+(\frac{Qt}{b})^a} \quad (6)$$

where $b = q_0 \times m/C_0$, C_0 is adsorbate concentration in the feed, Q is volumetric flow rate (ml/min), b is the volume of throughput required to achieve a half-maximum response,

a - Slope of regression function, q_0 - Equilibrium adsorption capacity, m - the mass of adsorbent.

These results were fitted using different theoretical adsorption models and illustrated in Figures 6-8. These breakthrough curves were plotted by taking C_t/C_0 on the y axis and time (min) on the x axis. Figure 6a shows the comparison of three theoretical models, Thomas, Bohart–Adams, Clark, and Figure 6b shows the comparison of Wolborska, Yoon–Nelson, and Yan models for different flow rates. Figures 7 and 8 also compare these models with experimental data for different bed heights and different influent concentrations, respectively.

Parameter evaluation and analysis

Each adsorption model contains one or more parameters in the equation that must be determined through model fitting.

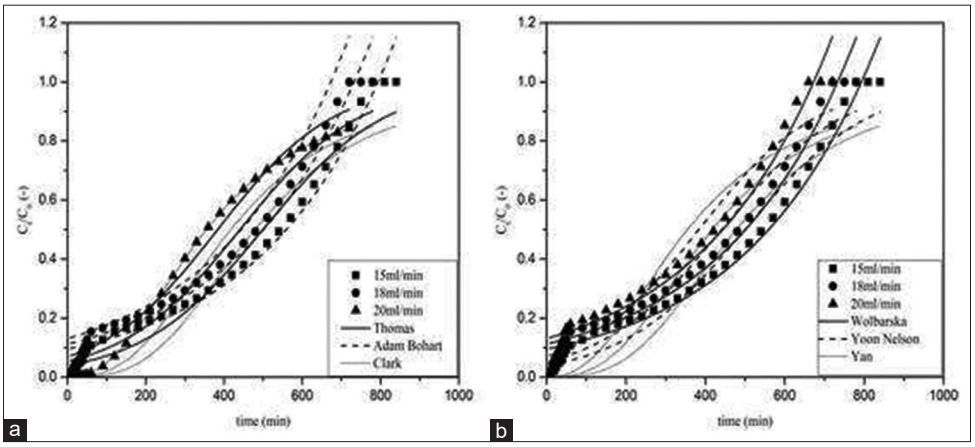

Figure 6: C_t/C_0 versus time for different initial flow rate of influent stream ([a] fit of Thomas Model, Adam Bohart Model, Clark Model and [b] fit of Wolbarska Model, Yoon–Nelson model and Yan Model)

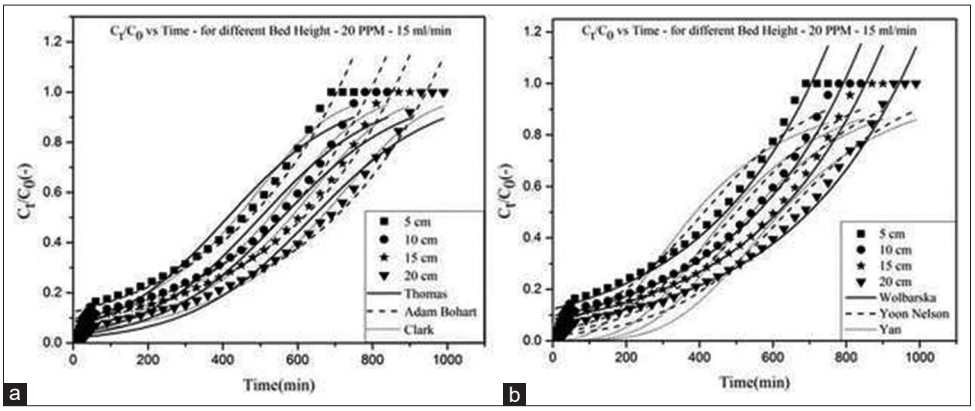

Figure 7: C_t/C_0 versus time for different bed heights of adsoprtion column ([a] fit of Thomas Model, Adam Bohart Model, Clark Model and [b] fit of Wolbarska Model, Yoon–Nelson Model and Yan Model)

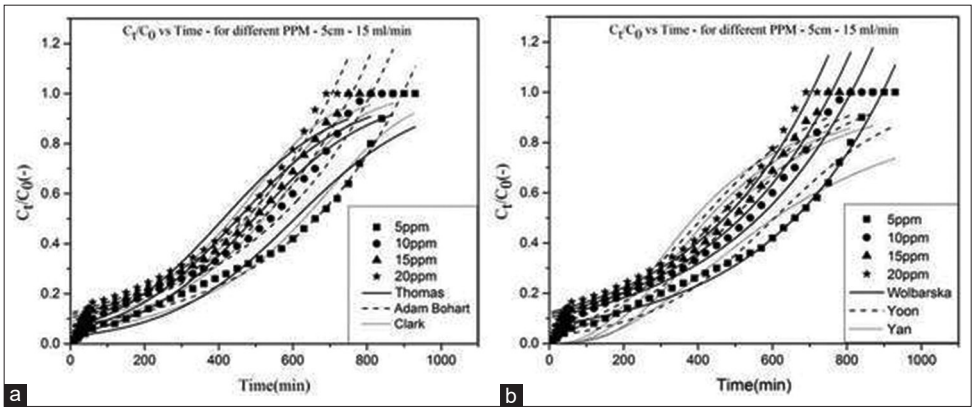

Figure 8: C_t/C_0 versus time for different influent concentrations ([a] fit of Thomas Model, Adam Bohart Model, Clark Model and [b] fit of Wolbarska Model, Yoon–Nelson Model, and Yan Model)

Tables 1 and 2 tabulate the parameters and their regression coefficients for different cycles, respectively. The variations of the parameters with respect to operating conditions are discussed below.

Each parameter has its physical significance and can be affected by changes made to the process. Every model includes a rate constant, which is influenced by mass transfer theories. While these constants do not have a specific significance, they can be influenced by changes in the process conditions.

Regeneration of adsorbent

Regeneration is a process of removing accumulated adsorbate from the saturated adsorbent.

Batch adsorption experiments were conducted under optimal conditions with 10 ppm fluoride water; after the adsorption process, the adsorbent was filtered out and dried. Further, the adsorbent was regenerated to avoid the purchasing of a new adsorbent every time. Regeneration of adsorbent was performed by using different normalities of NaOH (0.2N, 0.4N, 0.6N, 0.8N, 1N, and 1.2N). The fluoride-saturated adsorbent was suspended in 50 ml NaOH and shacked by a shaker at 200 RPM for 120 min. Again, the adsorbent was filtered out from the solution and dried for use in the adsorption process.

Regeneration studies were conducted to determine the extent of the adsorbent's reusability. Initially, the regeneration process was conducted with different concentrations of NaOH (0.2N, 0.4N, 0.6N, 0.8N, 1N, and 1.2N) to know a better concentration for the removal of adsorbate on the adsorbent.

Discussion

Column data analysis

From Figure 3, as the flow rate increased, the contact time between the adsorbent and the adsorbate decreased; this, in turn, reduced the bed's adsorption capacity and service time. This phenomenon is consistent with other research findings in the literature.[11]

From Figure 4, at the lowest bed depth, i.e. 5 cm, fluoride ions may not have enough time to diffuse into the holes of the dolomite powder, resulting in a shorter service time. This observation is consistent with the expected behavior of adsorption processes, where a longer contact time between the adsorbent and the adsorbate results in higher adsorption capacity and longer service time.

In contrast, sharper breakthrough curves were observed at higher influent concentrations. These results demonstrate

Table 1: Thomas, Bohart–Adams, and Clark model parameters

C_0 (mg/L)	Q (mL/min)	Z (cm)	Thomas model			Bohart–Adams model			Clark model		
			K_{Th} (mL/min mg)	q_0 (mg/g)	R^2	K_{BA} (mL/min mg)	N_0 (mg/mL)	R^2	A (−)	r (min)	R^2
5	15	5	1.157	5.091	0.96	0.590	37.60	0.99	4837.84	0.0106	0.971
10	15	5	0.6356	6.7008	0.97	0.278	68.17	0.97	2233.16	0.0113	0.982
15	15	5	0.4265	9.1614	0.97	0.198	88.72	0.97	1388.76	0.0114	0.981
20	15	5	0.3238	11.148	0.96	0.149	118.30	0.97	948.55	0.0116	0.989
20	15	10	0.3213	10.412	0.97	0.148	66.50	0.98	2545.76	0.0115	0.982
20	15	15	0.3128	9.334	0.97	0.146	47.74	0.98	4165.58	0.0112	0.983
20	15	20	0.3045	8.710	0.98	0.142	39.62	0.98	8152.71	0.0108	0.976
15	15	15	0.4261	6.4215	0.97	0.198	33.30	0.97	2503.48	0.0114	0.984
15	18	15	0.4352	6.8046	0.97	0.199	30.77	0.97	1401.59	0.0116	0.983
15	20	15	0.4503	6.5780	0.97	0.202	28.24	0.96	809.76	0.0119	0.975

Table 2: Yan, Wolborska, and Yoon–Nelson model parameters

C_0 (mg/L)	Q (mL/min)	Z (cm)	Yan model			Wolborska model			Yoon–Nelson model		
			q_0 (mg/g)	a (−)	R^2	β_a (min − 1)	N_0 (mg/mL)	R^2	q_0 (mg/g)	a (−)	R^2
5	15	5	5.129	2.407	0.96	22.188	37.60	0.98	0.00578	605.47	0.988
10	15	5	6.4286	3.047	0.995	18.986	68.17	0.97	0.00637	495.65	0.976
15	15	5	8.749	2.801	0.993	18.186	88.72	0.97	0.0064	451.96	0.974
20	15	5	10.607	2.596	0.993	17.603	118.30	0.97	0.00648	412.48	0.984
20	15	10	13.1696	3.288	0.994	9.856	66.50	0.98	0.00643	499.79	0.982
20	15	15	10.0616	3.628	0.994	6.962	47.74	0.98	0.00626	558.03	0.981
20	15	20	8.4781	3.888	0.995	5.615	39.62	0.98	0.00609	638.68	0.975
15	15	15	6.6434	3.103	0.995	6.592	33.30	0.97	0.00639	499.46	0.983
15	18	15	6.9560	2.762	0.994	6.141	30.78	0.97	0.00653	441.04	0.971
15	20	15	6.5672	2.373	0.994	5.705	28.24	0.96	0.0068	383.72	0.988

that changes in the concentration gradient can affect the saturation rate and breakthrough time, which is consistent with the findings of other studies. This phenomenon can be attributed to the fact that as the fluoride concentration increases; more adsorption sites become occupied, leading to a faster saturation of the adsorbent and a shorter breakthrough time.

Parameter evaluation and analysis

Adsorption capacity (q_0)

Adsorption capacity is the amount of adsorbate adsorbed on the unit mass of the adsorbent.[12]

q_0 = mass of adsorbate removed/mass of adsorbent.

Increasing the height of the adsorbent bed can lead to a reduction in adsorption capacity. This is because an increase in bed height corresponds to an increase in the mass of the adsorbent, which in turn can result in a decrease in the removal amount per unit mass of adsorbent due to the uniform distribution of the same amount of adsorbate. Experimental results have also demonstrated a similar variation of adsorption capacity with bed height.

An increase in the influent concentration of fluorine can lead to an increase in the amount of fluorine captured per unit mass of adsorbent, resulting in an increase in adsorption capacity. However, from experimental results, there is no significant variation in adsorption capacity with changes in the flow rate of the influent. This parameter is observed in both the Thomas and Yan models, and their variation is observed to be the same in both models.

Saturation concentration (N_0)

The saturation concentration refers to the maximum quantity of a substance that can dissolve in a standard volume of a particular solvent phase. In this context, it refers to the outlet concentration of the effluent stream after the bed has reached its saturation level. The saturation concentration is expressed in units of concentration that are the same as those used for the influent and effluent streams.[13]

An increase in the influent concentration of fluoride can lead to a quicker saturation of the adsorbent bed, resulting in a higher concentration of the effluent stream. Consequently, the saturation concentration also increases with the influent concentration. On the other hand, an increase in the flow rate can cause the adsorbent bed to become saturated more quickly, leading to a lower outlet concentration. As a result, the saturation concentration decreases with the flow rate.

An increase in the height of the adsorbent bed can lead to a higher saturation capacity, allowing for more adsorption in the bed and leading to a lower concentration of fluoride in the effluent stream. Consequently, the saturation concentration decreases as the bed height increases. Experimental results confirm that changes in the influent concentration, bed height, and flow rate of the influent can all affect the saturation concentration similarly.[14]

Time constant (τ)

The time required for a 50% adsorption breakthrough is the time measured at the outlet of the fixed bed for the effluent adsorptive concentration to reach 50% of its influent value. This parameter has units of time. As the flow rate of the influent increases, the contact time between the adsorbent and the influent decreases, this leads to a decrease in the time required for 50% breakthrough. However, the last sentence could be revised to say that experimental results show that the time constant increases with an increase in influent concentration and adsorbent bed height.[15]

Rate constants

Each unsteady-state model has a parameter that describes the adsorption rate, which is first-order in some models and second-order in others. The Thomas model has a rate constant that remains unchanged with increasing influent flow rate and adsorbent bed height, but it decreases with increasing influent concentration. On the other hand, the Bohart–Adams rate constant is not affected by flow rate or bed height, but it decreases as the influent concentration increases. Unlike the other models, the rate constant from the Yoon–Nelson model shows no significant changes with variations in influent concentration, bed height, or flow rate.[16]

Error analysis

Error analysis between experimental results and model results has been done using different predefined error functions mentioned below.

Standard square error is expressed as:

$$SSE = \frac{\sum_{i=1}^{N}\left[\left(\frac{C_t}{C_0}\right)_e - \left(\frac{C_t}{C_0}\right)_c\right]^2}{N}$$

where N is the number of data points, the subscripts "c" and "e" indicate calculated and experimental values, respectively.

HYBRID error is expressed as:

$$HYBRID = \frac{100}{p}\sum_{i=1}^{N}\left[\frac{\left(\frac{C_t}{C_0}\right)_e - \left(\frac{C_t}{C_0}\right)_c}{\left(\frac{C_t}{C_0}\right)_e}\right]^2$$

Marquardt's percent standard deviation is expressed as

$$MPSD = \sqrt{\frac{1}{N-p}\sum_{i=1}^{N}\left[\frac{\left(\frac{C_t}{C_0}\right)_e - \left(\frac{C_t}{C_0}\right)_c}{\left(\frac{C_t}{C_0}\right)_e}\right]^2}$$

P is number of parameters in the model

Average percentage error (Avg %) is expressed as:

$$\text{Avg}\% = \frac{\sum_{i=1}^{N} \frac{\left(\frac{C_t}{C_0}\right)_e - \left(\frac{C_t}{C_0}\right)_c}{\left(\frac{C_t}{C_0}\right)_e}}{N} \times 100$$

Sum of absolute errors is expressed as:

$$SAE = \sum_{i=1}^{N} \left(\frac{C_t}{C_0}\right)_e - \left(\frac{C_t}{C_0}\right)_c$$

Errors from these models are calculated and tabulated in Tables 3-5.

The acceptable method of determining the best-fitting model for the given experimental data is to use error analysis. The best fit for a model is defined by high values of R^2 and low error function values. From the above tables, obtained errors are in a considerable range for every model from every error function which indicates all the models as the best fit for the experimental data. The lowest of all the errors is given by the Clark model.

Regeneration of adsorbent

From Figure 9, it is observed that, at 1 Normality, the desorption rate is high and is found to be 95%. A regenerated adsorbent was used for the adsorption process and again new saturated adsorbent was regenerated. This cycle was continued until the outlet water is contained within the permissible limit of fluoride in it.[17,18]

From Figure 10 it was observed that water had 0.5 mg/L residual fluoride in it for the fresh adsorbent. After the first cycle, the residual fluoride was found to be 0.8 mg/L and it rose to 1.5 mg/L after three cycles. Further, after the 4th cycle, the residual fluoride content was found to be 2 mg/L, which is higher than the allowable permissible limits according to the WHO.

From Figure 11, it is observed that the adsorption capacity of the adsorbent was decreasing with the increase in the number of cycles due to the chemisorption of fluoride on the adsorbent.

$$\text{Adsorption efficiency} = \frac{C_0 - C_t}{C_t} \times 100$$

Table 3: Error analysis for Thomas and Bohart–Adams models

C_0 (mg/L)	Q (mL/min)	Z (cm)	Thomas model					Bohart–Adams model				
			Error square	Hybrid	MPSD	AVG %	SAE	Error square	Hybrid	MPSD	AVG %	SAE
5	15	5	0.0036	0.0900	0.3000	25.115	1.864	0.0013	1.1970	0.3000	55.42	1.20
10	15	5	0.0028	0.9887	0.9943	46.977	1.747	0.0036	8.9843	0.9943	126.56	1.93
15	15	5	0.0026	0.5967	0.7725	37.382	1.643	0.0030	5.0093	0.7725	80.50	1.63
20	15	5	0.0033	0.4852	0.6966	35.815	1.761	0.0026	2.3716	0.6966	59.93	1.37
15	15	15	0.0031	0.6172	0.7856	43.367	1.757	0.0025	5.3929	0.7856	105.04	1.55
15	18	15	0.0032	0.8313	0.9118	45.208	1.747	0.0029	5.9054	0.9118	91.56	1.60
15	20	15	0.0034	1.4401	1.2358	51.898	1.728	0.0035	5.9862	1.2359	95.17	1.66
20	15	5	0.0033	0.4852	0.6966	35.815	1.761	0.0026	2.3716	0.6966	59.93	1.37
20	15	10	0.0032	0.2577	0.5077	31.046	1.808	0.0021	2.4811	1.5751	63.63	1.30
20	15	15	0.0033	0.3344	0.5783	33.805	1.915	0.0018	3.7939	1.9478	71.33	1.16
20	15	20	0.0024	1.1462	1.0706	55.303	1.682	0.0017	19.008	5.3598	175.06	1.32

MPSD: Marquardt's percent standard deviation, SAE: Sum of absolute error, AVG %: Average precentage

Table 4: Error analysis for Yoon–Nelson and Yan models

CO (mg/L)	Q (mL/min)	Z (cm)	Yoon–Nelson model					Yan model				
			Error square	Hybrid	MPSD	AVG %	SAE	Error square	Hybrid	MPSD	AVG %	SAE
5	15	5	0.0036	0.0900	0.3000	25.115	1.864	0.0092	0.3909	0.6263	47.592	2.809
10	15	5	0.0028	0.9886	0.9943	46.975	1.747	0.0073	0.4443	0.6665	50.949	2.910
15	15	5	0.0026	0.5967	0.7725	37.382	1.643	0.0081	0.4410	0.6641	50.493	2.987
20	15	5	0.0033	0.4852	0.6966	35.815	1.761	0.0102	0.4438	0.6662	52.134	3.184
15	15	15	0.0031	0.6171	0.6515	43.363	1.757	0.0077	0.4615	0.6793	52.325	2.877
15	18	15	0.0032	0.8313	0.6437	45.208	1.748	0.0089	0.4493	0.6703	51.266	2.977
15	20	15	0.0034	1.4401	0.6266	51.898	1.728	0.0102	0.4029	0.6537	49.698	3.044
20	15	5	0.0033	0.4852	0.6966	35.815	1.761	0.0101	0.4438	0.6662	52.134	3.184
20	15	10	0.0032	0.2578	0.5077	31.046	1.808	0.0082	0.4722	0.6872	53.284	3.084
20	15	15	0.0033	0.3344	0.5783	33.805	1.915	0.0077	0.4826	0.6947	55.269	3.123
20	15	20	0.0024	1.1462	1.0706	55.303	1.682	0.0056	0.4774	0.6910	53.558	2.676

MPSD: Marquardt's percent standard deviation, SAE: Sum of absolute error, AVG %: Average precentage

Table 5: Error analysis for Clark and Wolborska models

C_0 (mg/L)	Q (mL/min)	Z (cm)	Clark model					Wolborska model				
			Error square	Hybrid	MPSD	AVG %	SAE	Error square	Hybrid	MPSD	AVG %	SAE
5	15	5	0.0019	0.3992	0.6318	35.758	1.483	0.0013	1.1965	1.0939	55.388	1.20
10	15	5	0.0016	2.9918	1.7296	73.439	1.435	0.0036	8.9723	2.9954	126.47	1.92
15	15	5	0.0014	1.5103	1.2289	50.418	1.243	0.0030	5.0103	2.0026	80.565	1.63
20	15	5	0.0018	1.0243	1.0121	42.798	1.333	0.0028	2.3713	1.5403	59.935	1.37
15	15	15	0.0017	1.9438	1.3942	65.746	1.413	0.0025	5.3951	2.3227	105.06	1.54
15	18	15	0.0019	1.9936	1.4119	60.666	1.419	0.1567	5.9292	2.2202	127.84	1.31
15	20	15	0.0022	2.7579	1.7103	66.248	1.431	0.0035	5.9839	2.5192	95.158	1.66
20	15	5	0.0018	1.0243	1.0121	42.798	1.333	0.0028	2.3713	1.5403	59.935	1.37
20	15	10	0.0015	0.8164	0.9035	40.124	1.283	0.0021	2.4808	1.5751	63.625	1.30
20	15	15	0.0014	1.2199	1.1045	45.475	1.304	0.0018	3.7928	1.9475	71.327	1.16
20	15	20	0.0010	5.9925	2.4479	100.76	1.194	0.0017	19.061	5.3659	175.31	1.32

MPSD: Marquardt's percent standard deviation, SAE: Sum of absolute error, AVG %: Average precentage

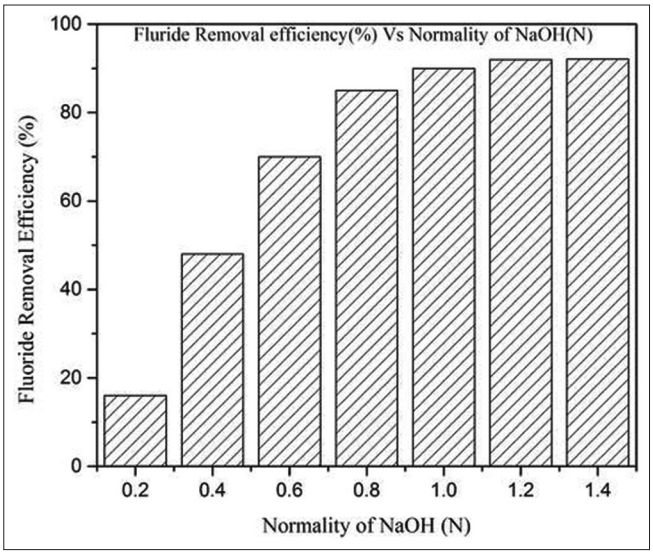

Figure 9: Fluoride removal efficiency versus normality of. NaOH

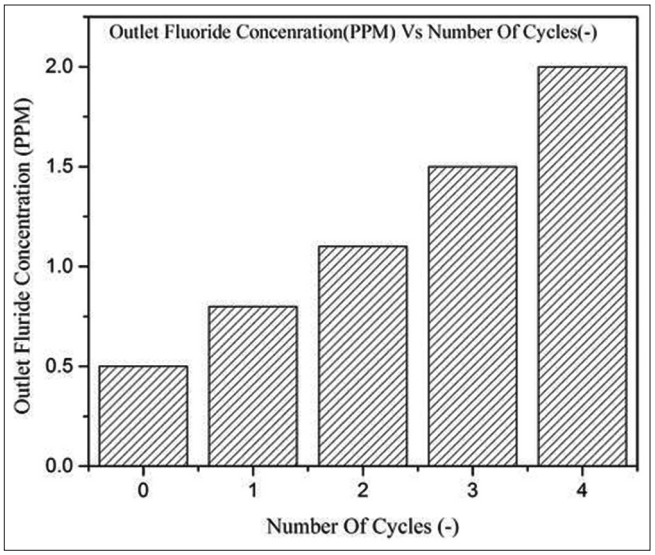

Figure 10: Fluoride ppm out in the processed water versus number of cycles

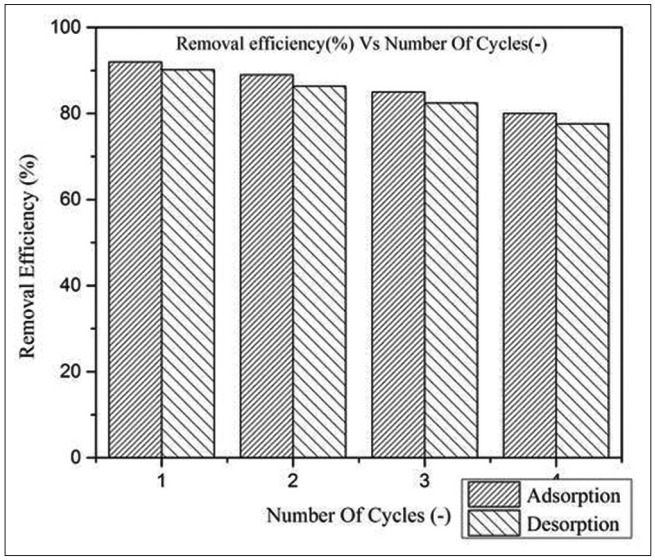

Figure 11: Adsorption and desorption efficiency of fluoride versus number of cycles

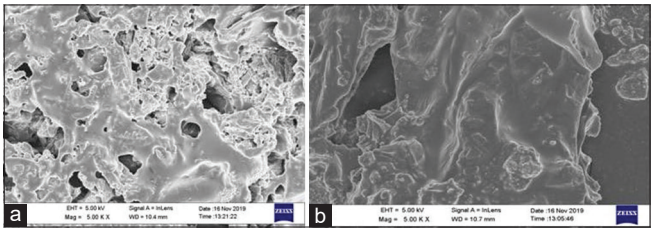

Figure 12: (a and b) Field emission scanning electron microscopy micrographs images of thermally treated dolomite powder before and after adsorption of fluoride ion onto its surface, respectively

$$\text{Desorption efficiency} = \frac{m_2}{m_1}$$

where, C_0 = initial fluoride concentration in water, C_t = final fluoride concentration in water, m_2 = mass of fluorine in NaOH after desorption, and m_1 = mass of fluorine on adsorbent.[11]

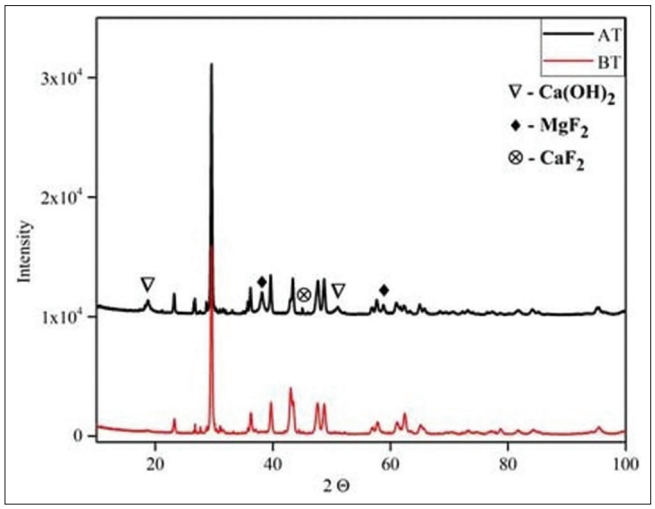

Figure 13: The X-ray diffraction patterns of the adsorbent (thermally treated dolomite powder) before and after being treated with fluoride solution

The decreasing trend for the adsorption efficiency was observed from the figure and up to the 3rd cycle, the fluoride content is within permissible limits. Hence, the adsorbent can be used three times for the adsorption process.

Field emission scanning electron microscopy analysis

The surface morphology of the adsorbent was investigated using a FE-SEM. FE-SEM micrographs were used to examine the morphological characteristics of before and after adsorption of adsorbents OPA, IGPA, and TTDP.

Figure 12a and b represents the FE-SEM surface micrograph of the TTDP adsorbents before and after adsorption, respectively. The surface texture of adsorbent (TTDP) has entirely changed after being treated with fluoride solution when compared to FE-SEM images of the adsorbents. The adsorbents that have been loaded with fluoride will have fluoride molecules covering the entire surface. After the fluoride ion adsorption, the pores were filled with fluoride molecules and were smooth. This result suggests that the functional groups inside the pores are where fluorine is adhering. The surfaces of the adsorbents grew smooth throughout the fluoride adsorption process. The surface becomes smoother as a result of fluoride adhering to the pores of the adsorbent. It is also possible that this has to do with the reduced surface heterogeneity of the adsorbent.

X-ray diffraction analysis

The XRD pattern of BT and AT samples is shown in Figure 13. The diffraction pattern of (BT) was determined to be Dolomite, $CaMg(CO_3)_2$ single phase with lattice parameters $a = b = 4.965$,[2] $c = 16.90$,[1] and $\alpha = \beta = \gamma = 120$ and the diffraction pattern of AT, on the other hand, indicated a mixed phase with $CaCO_3$ as the majority phase. In AT, five minor phases, $Ca(OH)_2$ (18.76, 51.03), MgF_2 (38.14, 58.77), and CaF_2 (45.00), were identified in addition to the primary phase and are indicated in the diffraction pattern. These results show that the F-element in water interacts with Mg and Ca in adsorbent and forms minor phases such as MgF_2, CaF2, and $Ca(OH)_2$ and major phase as $CaCO_3$.

Conclusions

Our experiments deduce that fluoride using treated dolomite powder in a packed adsorption column is an efficient and feasible method. From column studies, we investigated the behavior of breakthrough curves with varying flow rate, initial fluoride concentration, and bed height. Breakthrough time increases with a low flow rate (15 m/min), low influent concentration (5 ppm), and higher bed depth (20 cm). The parameters of different theoretical models are estimated by using fixed-column experimental data. Almost all models are well fitted. Batch regeneration of adsorbent studies is carried out with NaOH solution. It showed up to three cycles we can regenerate the adsorbent.

Acknowledgements

The authors would like to express their gratitude to Rajiv Gandhi University of knowledge and Technologies and JNTU Anathapur.

Financial support and sponsorship

Nil.

Ethics Code

We believe our manuscript does not require ethical clearance as it does not involve human subjects or sensitive data. We have ensured compliance with all relevant ethical guidelines and regulations applicable to our research field.

Conflicts of interest

There are no conflicts of interest.

Authors' Contributions

Chinthayyanaidu Rudram designed the equipment, conducted the experiments, and wrote the manuscript. P. Dinesh Shankar Reddy analyzed the data and results, and provided corrections to the manuscript.

References

1. World Health Organization. Fluorides and Human Health. Ser. 59. Geneva: World Health Organization Publication Monography; 1970.
2. Guangyu Y, Viraraghavan T, Min C. A New model for heavy metal removal in a biosorption column. Adsorp Sci Technol 2000;19:25-43.
3. UNICEF. Learning from Experience. Water and Environmental Sanitation in India. New York: The United Nations Children's Fund (UNICEF); 2002.
4. Poonam M, Suja G. A review on adsorbent used for defluoridation of drinking water, Reviews in Environmental Science and Bio/Technology 2014;14:195-210.
5. Tatsuro N, Tsurunaga K, Takeshi K. Insoluble treatment with dolomite based material for the fluoride ion, Key Engineering Materials 2014; 617:28 31.
6. Rudram C, Praveen LP, Reddy PD. Comparative adsorbent studies using pyrolysed materials prepared from custard apple (annona squamosa) leaves in removal of fluoride from waste water. Asian J Chem 2022;34:2597-603.
7. Marina T, Nediljka VM, Jevena P. Application of mathematical empirical

models to dynamic removal of lead on natural zeolite clinoptilolite in a fixed bed column. Indian J Chem Technol 2011;18:123-31.
8. Kanyora AK, Kinyanjui TK, Kariuki SM, Chepkwony CK. Efficiency of various sodium solutions in regeneration of fluoride saturated bone char for de- fluoridation. IOSR J Environ Sci Toxicol Food Technol 2014;8:10-6.
9. Swaroop B, Umesh M. Continuous fixed-bed column study and adsorption modeling: Removal of lead ion from aqueous solution by charcoal originated from chemical carbonization of rubber wood Sawdust, Hindawi. J Chem 2015:1-8.
10. Rafique A, Awan MA, Wasti A, Qazi IA, Arshad M. Removal of fluoride rom drinking water using modified immobilized activated alumina. J Chem 2013:1-7.
11. Mendoza-Castillo DI, Reynel-Avila HE, Bonilla-Petriciolet A, Silvestre-Alber J. Synthesis of denim waste-based adsorbents and their application in water defluoridation. J Mol Liq 2016;221:469-78.
12. Dhiraj M, Poonam M, Suja G. Utilization of marble waste powder as a novel adsorbent for removal of fluoride ions from aqueous solution. J Environ Chem Eng 2016;4:932-48.
13. Jianguo C, Yanyang Z, Bingcai P, Weiming Z, Lu L, Quanxing Z, "Efficient defluoridation of water using reusable nanocrystalline layered double hydroxides impregnated polystyrene anion exchanger", Water Research, 2016; 102: 109-116.
14. Tej PS, Apoorva T, Deepankar DP, Majumder CB. Effect of co-existing ions on defluoridation capacity of Java plum seeds. World J Pharm Pharm Sci 2016;9:320-7.
15. Jitu S, Susmita S, Tobiul HA, Paran JK, Rajib LG. Removal of toxic fluoride ion from water using low cost ceramic nodules prepared from some locally available raw materials of Assam, India. J Environ Chem Eng 2017;5:2488-97.
16. Zhang J, Kong Y, Yang Y, Chen N, Feng C, Huang X, *et al.* Fast capture of fluoride by anion-exchange zirconium-graphene hybrid adsorbent. Langmuir 2019;35:6861-9.
17. Tong LT, Poovarasi A, Krusnamurthy P, Nakajima H, Rashid SA, Adsorptive, kinetics and regeneration studies of fluoride removal from water using zirconium-based metal organic frameworks, 2020; 18740-52.
18. Yujian Z, Lizhi H, Guoqiao W, Xinxin Z, Ya L, Yao C. Defluorination and regeneration study of lanthanum doped sewage sludge based activated carbon. J Environ Chem Eng 2021; 9:1 9.